HHS Public Access

Author manuscript

J Immunol. Author manuscript; available in PMC 2016 June 15.

Published in final edited form as:

J Immunol. 2015 June 15; 194(12): 5692–5702. doi:10.4049/jimmunol.1402736.

Concordance of Increased B1 Cell Subset and Lupus Phenotypes in Mouse and Human Dependent on BLK Expression Levels

Ying-Yu Wu[*], **Ina Georg**[†], **Alejandro Díaz-Barreiro**[†], **Nieves Varela**[†], **Bernard Lauwerys**[‡], **Ramesh Kumar**[*], **Harini Bagavant**[*], **Mireia Castillo-Martín**[§], **Fadi El Salem**[§], **Concepción Marañón**[†], and **Marta E. Alarcón-Riquelme**[*,†]

[*]Arthritis and Clinical Immunology Program, Oklahoma Medical Research Foundation, Oklahoma City, OK 73112, USA

[†]GENYO. Centre for Genomics and Oncological Research Pfizer / University of Granada / Andalusian Regional Government, PTS Granada, 18016, Spain

[‡]Pôle de Pathologies Rhumatismales, Institut de Recherche Expérimentale et Clinique, Université Catholique de Louvain, Belgium

[§]Department of Pathology, Icahn School of Medicine at Mount Sinai, New York, NY 10029, USA

Abstract

Polymorphisms in the *BLK* gene have been associated with autoimmune diseases, including systemic lupus erythematosus (SLE), with risk correlating with reduced expression of *BLK*. How reduced expression of *BLK* causes autoimmunity is unknown. Using $Blk^{+/+}$, $Blk^{+/-}$, and $Blk^{-/-}$ mice, we show that aged female $Blk^{+/-}$ and $Blk^{-/-}$ mice produced higher anti-dsDNA IgG antibodies and developed immune complex-mediated glomerulonephritis, compared to $Blk^{+/+}$ mice. Starting at young age, $Blk^{+/-}$ and $Blk^{-/-}$ mice accumulated increased numbers of splenic B1a cells, which differentiated into class-switched $CD138^{+}$IgG-secreting B1a cells. Increased infiltration of B1a-like cells into the kidneys was also observed in aged $Blk^{+/-}$ and $Blk^{-/-}$ mice. In human, we found that healthy individuals had *BLK* genotype-dependent levels of anti-dsDNA IgG antibodies as well as increased numbers of a B1-like cell population, $CD19^{+}CD3^{-}CD20^{+}CD43^{+}CD27^{+}$, in peripheral blood. Furthermore, we describe the presence of B1-like cells in the tubulointerstitial space of human lupus kidney biopsies. Taken together, our study reveals a previously unappreciated role of reduced *BLK* expression on extraperitoneal accumulation of B1a cells in mice, and the presence of IgG autoantibodies and B1-like cells in human.

Correspondence: Ying-Yu Wu, Arthritis and Clinical Immunology, Oklahoma Medical Research Foundation: ying-yu-wu@omrf.org; Marta E. Alarcón-Riquelme, Arthritis and Clinical Immunology, Oklahoma Medical Research Foundation: alarconm@omrf.org and marta.alarcon@genyo.es.

Disclosures

The authors have declared that no conflict of interest exists

Introduction

Systemic lupus erythematosus (SLE) is a chronic inflammatory condition with an autoimmune etiology caused by the interplay of several genes and environmental factors. In recent years, many susceptibility genes for lupus have been identified (1, 2). A genome-wide association study (GWAS) found a single-nucleotide polymorphism (SNP) in the 5' upstream region of the B Lymphoid Tyrosine Kinase (BLK) gene associated with SLE (3). Multiple studies have confirmed the association of SNPs in the promoter of *BLK* with SLE in several populations (4, 5). *BLK* is also associated with other autoimmune disorders, such as rheumatoid arthritis (RA) (6), systemic sclerosis (SSc) (7), Sjögren's syndrome (8, 9), primary anti-phospholipid syndrome (APS) (10), dermatomyositis (11) and Kawasaki disease (12). The SNP risk alleles found in regulatory regions have been shown to associate with reduced mRNA levels of *BLK* and reduced protein expression (3, 13–15).

BLK encodes a non-receptor member of the Src family of tyrosine kinases (SFKs). BLK is mainly expressed by B lymphocytes but also, to a lesser extent by non-B-cell lineages, such as plasmacytoid dendritic cells (pDCs), pancreatic β-cells, and γδT cells (13, 16–19). Though Blk phosphorylation is detectable upon anti-IgM stimulation (20–22), BLK expression is downregulated upon BCR stimulation (15), suggesting that BLK may play a dual role downstream of BCR signaling.

Early studies from gene targeted mice showed that the *Blk* KO mouse did not have significant phenotypes that would make *Blk* necessary for B cell activation (23). Revisiting immune phenotypes in the *Blk* knockout mouse in the C57BL/6 background revealed a role for *Blk* in the production of higher levels of anti-nuclear antibodies (ANAs), increased B1a cell numbers in the peritoneal cavity, and the presence of hyper-responsive marginal zone B (MZ B) cells (24).

Expansion of B1 cells and their contribution to lupus pathogenesis was reported in several lupus-prone mouse models, and additionally in some mice deficient in genes encoding negative regulators in BCR signaling (25, 26). In mice, B1 cells include B1a ($CD5^+$) and B1b ($CD5^-$) subsets. B1b cells are mainly responsive to T cell-independent antigens, while B1a cells can secrete polyreactive IgM natural antibodies or even IgG autoantibodies when found extraperitoneally (27–29).

Recently, a population of B1 cells in human was described in adult peripheral blood and umbilical cord with the $CD20^+CD27^+CD43^+CD70^-$ phenotype. These cells have the capacity of stimulating T cells efficiently, producing IgM spontaneously, and show tonic intracellular signaling. They are, in this respect, similar to mouse B1 cells (30). Even though their nature is still a matter of controversy (31–35), this population is expanded in SLE patients (36), while it is decreased in human common variable immunodeficiency patients (37).

It is still largely unknown how risk alleles of *BLK* or its reduced expression promote abnormalities that lead eventually to autoimmunity. We therefore utilized *Blk*+/+, *Blk*+/− and *Blk*−/− mice, representing differential expression levels of *Blk* mRNA and BLK protein (24), and performed a comprehensive analysis of their phenotypes to investigate if these

animals develop any kidney disease. In parallel, we investigated several peripheral blood cell populations of healthy human donors genotyped for the human SNP rs2736340 in the promoter region of the *BLK* gene (3).

Both in mice and humans, we describe a *BLK* genotype-dependent increase of B1a and B1-like cells, respectively, and the association with high levels of IgG anti-dsDNA antibodies in serum. We also find immune complex-mediated glomerulonephritis in *Blk*-deficient mice with increased infiltration of B1a-enriched cells into the kidneys. We then make the unprecedented observation of the presence of double positive $CD20^{+}CD43^{+}$ B1-like cells in renal biopsies from lupus nephritis patients. Intriguingly, female lupus patients bearing *BLK* risk alleles had earlier age at onset of lupus nephritis. Our results support a role for BLK in controlling the size of the B1a/ B1-like cell pool, the redistribution of B1a/ B1-like cells and the development of lupus nephritis.

Materials and Methods

Mice

Blk KO mice were a generous gift from Dr. Susan Hayes (State U of Upper New York, NY). *Blk* mice were backcrossed 9–10 generations to C57BL/6J mice. All mice were maintained under specific pathogen-free conditions at Oklahoma Medical Research Foundation (OMRF). All animal procedures were approved by the IACUC at OMRF.

Human study population and genotyping

Blood samples in EDTA and serum samples were obtained from healthy donors previously genotyped for *BLK* SNP rs2736340, in the BLK promoter (3), using ImmunoChip (Illumina). For this study 25 CC-, 9 CT- and 12 TT-allele donors were recruited. Male/ female ratios were similar in all the groups (35% for CC, 33% for CT and 36% for TT). There were no statistical differences in the age of the different genetic groups (median and [interquartile range] and these were 33 [24–63] for CC, 32 [27–49] for CT and 34 [28–58] for TT). For some patients only serum samples could be obtained and cytometry data could not be generated. The protocols were approved by the Ethical Committee of the Hospital “Virgen de la Macarena” for the Fundación Pública Andaluza Progreso y Salud in Seville.

Cell preparation, flow cytometry, cell sorting and antibodies

Mice were anesthetized by inhalation with isoflurane. To avoid contamination of lymphocytes in kidney blood vessels, perfusion was performed pumping 10 ml sterile PBS from the left ventricle, while the right atrium was opened with a small cut. Perfused kidneys were minced and resuspended in digestion buffer consisting of 2 mg/ml collagenase IV (Sigma-Aldrich) and DNase I (1 μg/ml) in RPMI complete media and incubated at 37°C for 45 min. Cells were centrifuged, filtered through a 70-μm cell strainer, and mixed 1:1 with 40% Percoll in 1X PBS. This was centrifuged at 3000 rpm for 20 min at room temperature without brake. The loose pellet was washed and cells were counted. Peritoneal lavage was collected after i.p. injection of 8–10 ml of sterile 1X PBS.

Single-cell suspensions from mouse spleens, the peritoneal cavity, and kidneys were incubated with fluorescently labeled antibodies (detailed in supplemental materials) after blocking nonspecific binding with anti-mCD16/32 (Clone: 2.4G2) or 10% rabbit serum (Sigma-Aldrich). Human B1-like, B2 cells and $CD19^+$B cells were quantified in whole blood by flow cytometry using no wash protocols, immediately after bleeding. 200 μl of whole blood in EDTA were treated with the indicated antibody-cocktails for 10 min at room temperature in the dark. Afterwards, erythrocytes were lysed using QuickLysis solution (Cytognos) following the manufacturer recommendations. Data were acquired on a LSR II or FACSVerse flow cytometer (BD) and analyzed using FlowJo 9.8 software (Tree Star). Antibody-labeled IgM^{hi} and $IgM^{lo/-}$ $CD138^+$ B1a cells from spleens, class-switched B1a cells and plasma cells from kidneys were sorted by FACSaria (BD).

Antibodies used for murine cells were as follows: anti-B220-PE-TexasRed or FITC (clone: RA3-6B2), anti-mCD93-PerCP.Cy5.5 (clone: AA4.1), anti-mCD23-eFluor660 or PE (clone: B3B4), anti-mCD21/CD35-PE/Cy7 (clone: 7E9), anti-mIgM-APC/Cy7 (clone: RMM-1), anti-mIgM- APC (clone: II/41), anti-mIgD-FITC or eF450 (11–26), anti-mCD5-PE or PerCPCy5.5 (clone: 53-7.3), anti-mouse and rat β1-integrin/CD29-Alexa-Fluor488 (clone: HMβ1-1), anti-mCD138-Brilliant Violet 421 (clone: 281-2), anti-CD19-PE/CF594 (clone: 1D3), anti-CD43-APC (clone: S11), anti-mCD11b-BV421 (clone: M1/70) , anti-mCD45.2-PE (clone: 104), and Arm. Hamster IgG isotype control-AF488 (clone: HTK888) were purchased from Biolegend, eBioscience or BD Bioscience. Antibodies and reagents used for human cells were as follows: CD43-FITC, CD27-APC, CD19-PerCP-eFuor710, CD20-PE-Cy7, CD3-APC-eFluor780 (eBioscience), CD29-PE (Immunotools), DRAQ7 (Beckman-Coulter), and CD70-PE (BD Biosciences).

Measurement of antibodies by ELISA

For IgG anti-dsDNA ELISAs, 96-well Maxisorp Immuno plates (Nunc) were coated with 500 μg/ml protamine sulphate (Sigma-Aldrich) for 45 minutes at 4°C and afterwards with calf thymus DNA (50 μg/ml) O/N at 4°C. After washing with PBS-T (0.05% Tween 20) the plates were blocked for 1h with 10% calf serum+ 5% goat serum in PBS-T prior to addition of diluted serum (1:2000 for human samples, 1:25 for *Blk* mouse samples, and 1:200 for B6.Sle1.yaa mouse samples) for 2h. Antibodies were detected using goat anti-mouse IgG-HRP (Southern Biotechnology) or goat anti-human IgG-HRP (Life Technologies), and peroxidase reactions were developed using OptEIA TMB substrate (BD). The reaction was stopped using 1N sulfuric acid and the absorbance at 450 nm was read using a spectrophotometer. In every plate serum from IgG anti-$dsDNA^+$ B6.Sle1.yaa mice or human lupus patient was included as a reference for normalizing purposes. The arbitrary units were calculated as the ratio OD_{450} (problem serum)/OD_{450} (reference serum). The concentration of total IgG and IgM in serum of genotyped healthy donors was quantified using “Human IgG ELISA quantitation kit” and “Human IgM ELISA quantitation kit”, respectively (Bethyl Lab).

ELISPOT assay

ELISPOT assay was carried out as previously described (38, 39). In brief, indicated numbers of sort-purified B1a cells and PCs or 5×10^4 splenocytes were distributed onto MultiScreen-

IP Plates (Millipore) pre-coated with goat anti-mouse IgG+M+A (H+L) cross absorbed antibodies (Bethyl Lab) and then incubated in RPMI 1640 containing 10% heat-inactivated fetal bovine serum, 2 mM L-glutamine, 50 μM 2-mercaptoethanol, 100 U/ml penicillin, and 100 μg/ml streptomycin for 4h at 37°C and 5% CO_2. Plates were treated with F(ab')2 fragment, goat anti-mouse IgG or anti-mouse IgM, HRP-conjugated, (Jackson ImmunoResearch), or goat anti-mouse IgG2c, HRP conjugated, (Bethyl Lab) and developed with AEC (2-amino-9-ethylcarbzole) substrate (Sigma-Aldrich). IgM-, IgG- and IgG2c-secreting B cells were enumerated using ImmunoSpot analyzer/software (Cellular Technology Limited).

Mouse histopathology and immunofluorescence staining

Mouse kidneys were fixed in 10% neutral buffered formalin and embedded in paraffin for histological and immunohistochemical analyses. Thereafter, specimens were dehydrated in an ascending ethanol series and embedded in paraffin for subsequent sectioning into 5–7 μm sections using a microtome (Leica). Three or four consecutive renal tissue sections were placed onto a slide for histological analyses. Mouse renal tissue sections were stained with H&E or Jones' methenamine silver-periodic acid-Schiff according to standard practices.

Two observers blinded to the experimental design evaluated histopathology. The severity of GN was scored as previously reported (40). In brief, renal pathology was evaluated for active proliferative changes in the glomerular mesangium, involvement of the peripheral capillary loops, extent of inflammatory cell infiltration and graded on a score of 0 (no pathology) to 4 (maximum pathology). Proliferative/acute GN was calculated as a weighted score (% glomeruli affected * mesangial score) + (% glomeruli affected* peripheral score*2). An average of 149±38 glomeruli were studied for each mouse. Chronic change indicated by glomerular sclerosis, fibrosis and tubular atrophy was also scored. GN severity results are presented as a sum of proliferative and chronic glomerular pathology.

Mouse kidneys were embedded in 1:1 TFM/OCT compounds and snap frozen in pre-chilled 2-methylbutane by dry ice. Then 10 μm sections were cut on a cyrostat, mounted on Superfrost Plus slides, and fixed at −20°C acetone for 2 min. After rehydration in staining buffer (1X PBS, 1% goat serum, 2% BSA), slides were stained with the following: IgG(H+L)-Cy3 (Jackson Immunoresearch), C3-FITC (Bethyl Lab). DAPI counterstain was applied to each slide before coverslip mounting. Images were acquired using Zeiss Axiovert 200M inverted fluorescent microscope and AxioVision software. Glomerular IgG and C3 depositions were quantified as described (41). In brief, 5 *Blk*+/+, 5 *Blk*+/− and 3 *Blk*−/− female mice at 1 yr of age were used. 5 random fields taken under FITC- and Cy3- channels of the confocal microscope were subjected to quantification from each mouse. In average, 20 glomeruli from each mouse were graded into 3 levels, 0-mild, moderate, and severe. After determining the percentage of IgG^+ or $C3^+$ glomeruli, individual scores and median percentages of glomeruli were represented in scattered dot and column plots.

Digital RT-PCR (dRT-PCR) and determination of *BLK* mRNA in $CD19^+$ B cells

Total RNA was isolated from 1×10^6 fresh peripheral blood mononuclear cells (PBMCs) of healthy donors using High Pure RNA Isolation Kit (Roche). *BLK* expression was measured

by relative quantification using QuantStudio™ 3D Digital PCR System with probes Hs01017452_m1 for BLK (FAM), and Hs001003268 for HPRT1 (VIC) normalizer using cDNA equivalent to 10 ng and 20 ng RNA. Fluorescence in QuantStudio™ 3D Digital PCR 20K Chips was measured by QuantStudio™ 3D Digital PCR Instrument and data were analyzed by QuantStudio™ 3D AnalysisSuite™ Cloud Software (Life Technologies). As *BLK* mRNA expression in $CD19^+$ B cells is at least 30-fold higher than in other BLK-expressing leukocytes (13), we have considered that the measured BLK expression comes mainly from B lymphocytes. Thus, the quantity of BLK mRNA measured by dRT-PCR was estimated using the formula: BLK expression in B lymphocytes = 100* BLK expression in PBMC / % $CD19^+$ cells in PBMCs. The frequency of $CD19^+$ B cells in the PBMCs was determined by FACS analysis.

Human lupus nephritis patients, renal biopsy preparation, and immunofluorescence staining

Paraffin-embedded specimens from renal biopsies, retrospectively obtained from thirteen patients diagnosed with SLE and lupus nephritis at Cliniques Universitaires Saint Luc, Brussel (Belgium) and paraffin tissue sections from a normal adult human kidney (BioChain, cat# T2234142), were used for immunofluorescence analyses. Patients were grouped according to the presence of non-risk (CC, n= 6) or risk (TT, n= 7) alleles of SNP rs2736340. Detailed clinical information was recorded including age, gender, disease manifestations, medical history and key laboratory parameters. Paraffin tissue sections mounted on slides were deparaffinized and rehydrated sequentially. After antigen retrieval, tissue sections were blocked with 5% normal goat serum (Vector Laboratories) and 5% normal human serum (PAA) together in PBS/0.3% Tween 20. Thereafter, CD20 and CD43 antigens were sequentially stained with the specific antibodies diluted in blocking buffer. For CD20, the first primary antibody, mouse antihuman CD20 Alexa Fluor®488 (clone L26, eBioscience) was applied on each slide at a 1:50 dilution followed by incubation with the secondary antibody, Alexa-Fluor®488 goat anti-mouse IgG (H+L) (Life technologies) at a 1:400 dilution. This step was performed to enhance the signal of the anti-human CD20 Alexa Fluor®488 primary antibody. After washing slides three times, the second primary antibody, monoclonal mouse IgG1, kappa anti-human CD43 (clone DF-T1, DakoCytomation) was applied at a 1:400 dilution followed by the Alexa Fluor®555 goat anti-mouse IgG_1 (γ1)-specific secondary antibody (Life technologies) at 1:200. Nuclei were counterstained using 300 nM DAPI solution (Life technologies) at room temperature for 5 min. After washing, slides were mounted in Mowiol® 4–88 (Sigma-Aldrich) containing 2.5% of the anti-fading reagent *p*-Phenylenediamine (Sigma-Aldrich). Slides were stored in the dark at 4°C. Confocal images were captured using a Zeiss LSM 510 laser scanning microscope equipped with the Zen imaging system. Double immunofluorescence staining was performed at least twice for each patient and the healthy control. Negative control was conducted to ensure that nonspecific staining in-between the two secondary antibodies was absent. For this, immunoreactions were done as described above omitting the mouse IgG1, kappa antihuman CD43. For unbiased quantification of $CD20^+$, $CD43^+$ and $CD20^+CD43^+$ cells, at least 10 fields were selected in the DAPI channel for each tissue section. The total number of each stained cell type / 0.01 mm^2 was calculated (Table 1).

Statistical analysis

Statistical significance among >2 groups was determined by Kruskal-Wallis nonparametric test with Dunn's multiple comparison. Statistical significance between 2 groups was determined by Mann-Whitney nonparametric test. Graphs and statistical analyses were performed using Prism 6.0 or 5.0 softwares (GraphPad). Values are reported as mean with or without SEM, or median with or without IQR (interquartile range).

Results

Aged Blk+/− and Blk−/− female mice spontaneously develop IgG anti-dsDNA antibodies and lupus nephritis

A corhort of *Blk*+/+, *Blk*+/−, and *Blk*−/− female mice was monitored for development of anti-dsDNA IgG and lupus nephritis. Sera were collected every 8–12 weeks starting at 24-wk through 48-wk of age. Anti-dsDNA IgG levels from *Blk*+/− and *Blk*−/− mice started to show a significant increase compared to *Blk*+/+ mice by week 48, but not earlier (data not shown) (Figure 1A). However, the level of anti-dsDNA IgG of *Blk*−/− mice is still much less than the level of lupus-prone B6.Sle1.yaa males (Figure 1A).

We then investigated the presence of kidney disease with hematoxylin and eosin (HE) and periodic acid-schiff (PAS) staining of paraffin-embedded kidneys from female mice over 1-year of age. *Blk*+/+ mice showed normal renal histology with occasional/ rare glomeruli showing mild mesangial changes. Some glomeruli from aged *Blk*+/− mice had become enlarged with hypercellularity (Figure 1B). However, glomeruli from *Blk*−/− kidneys showed enlarged and hypercellular glomeruli with significant mesangial expansion. Several inflammatory cell infiltrates were present in peri-glomerular regions (Figure 1B). Some mice showed dilated capillary loops containing intra-luminal hyaline deposits. Changes suggestive of focal glomerular sclerosis were seen in *Blk*−/− mice (data not shown).

According to quantification of glomerulonephritis (GN) severity, aged *Blk*+/− mice had slight but non-significant increase of GN severity index compared to aged *Blk*+/+ mice (Figure 1C). In contrast, aged *Blk*−/− mice had a significantly higher cumulative GN severity index compared to aged *Blk*+/+ or *Blk*+/− mice (Figure 1C). The GN severity was female related, as aged *Blk*−/− male mice rarely showed proliferative and chronic GN (data not shown). The tendencies towards increased complement 3 (C3) and IgG-deposition in glomeruli were confirmed in kidneys from aged *Blk*+/− and *Blk*−/− mice (Figure S1), implying the nephritis is mediated by immune complex (IC) deposition in the glomeruli.

Taken together, *Blk*+/− and *Blk*−/− mice are prone to spontaneously develop IgG anti-dsDNA antibodies. IC-mediated GN developed in female *Blk*−/− mice at old age.

Splenic B1a cells are increased in female Blk+/− and Blk−/− mice

Two groups of mice were setup for flow cytometry analysis: young mice (≤18-wk-old, males and females) and aged mice (≥52-wk-old, females only). Total splenocyte numbers were not affected, neither follicular (FO) B, marginal zone (MZ) B or transitional B cells (Figure S2 and data not shown). To compare the phenotypes among different *Blk* genotypes

or between young and aged groups of mice correspondingly, we only present data from females in all of the results below. We confirmed an increase of peritoneal B1a (PerC B1a) cells in young *Blk*−/− mice (Figure 2A & 2B) using the same gating strategy as previously (24). Interestingly, aged mice had at least, 10 times more PerC B1a cells than young mice (Figure 2B). However, enlarged PerC B1a cell pools in young *Blk*−/− mice disappeared in aged *Blk*−/− mice (mean values for aged mice: *Blk*+/+ [35.7], *Blk*+/− [70.1], *Blk*−/− [51.2], $p>0.05$) (Figure 2B).

B1a cells are only capable of secreting antibodies when they migrate to the spleen, BM or inflamed tissues, but not when residing in the peritoneal cavity (27–29). Since only aged female *Blk*+/− and *Blk*−/− mice developed autoimmunity and glomerulonephritis, we firstly tested whether splenic B1 cells accumulated in those *Blk*+/− or *Blk*−/− mice. We adopted FACS analysis strategies for splenic B1 cells from two different labs (28, 42, 43) and modified gating strategies to our study accordingly.

The first FACS gating strategy adopted from Baumgarth's group to characterize splenic B1a cells is $IgM^{hi}IgD^{int/lo}B220^{int/hi}CD5^{int}CD43^{+}CD23^{lo/-}$, while that for splenic B1b cells is $IgM^{hi}IgD^{int/lo}B220^{int/hi}CD5^{-}CD43^{+}CD23^{lo/-}$ (42). Aged *Blk*+/− and *Blk*−/− mice showed increased percentages of splenic B1a cells (Figure 2C). Absolute numbers of splenic B1a cells, but not B1b cells, were significantly increased in aged *Blk*+/− and *Blk*−/− mice, compared to aged *Blk*+/+ mice (Figure 2D) (mean values for aged mice: *Blk*+/+ [4.3], *Blk* +/− [6.9], *Blk*−/− [8.9]). However, *Blk* genotypes unlikely affected the numbers of splenic B1b cells from aged mice (Figure 2D).

Since alternative FACS antibody cocktails do not include anti-CD43, we could only characterize splenic B1a cells, and not splenic B1b cells (43). An alternative splenic B1a cell population was characterized as $B220^{int/hi}CD93^{-}IgM^{hi}IgD^{int/lo}CD23^{lo/-}CD21^{int/-}CD5^{int}$ (SP B1a I) (Figure S3A). Young *Blk*+/− and *Blk*−/− mice showed increased percentages of splenic B1a cells (Figure S3A). Absolute numbers of splenic B1a cells were significantly increased in young *Blk*+/− and *Blk*−/− mice, compared to *Blk*+/+ mice (Figure S3B). Aged mice showed a 3–7.5 fold-increase in splenic B1a cells, as compared to young mice with the same *Blk* genotypes (Figure S3B). Compared with aged *Blk*+/+ mice, aged *Blk*+/− and *Blk* −/− mice also had a significant increase in splenic B1a cells (mean values for aged mice: *Blk*+/+ [5.8], *Blk*+/− [13.8], *Blk*−/− [21.7]) (Figure S3B). Taken together, lack or reduction of *Blk* expression hastened splenic B1a cell accumulation with age.

Increased class-switched $CD138^{+}$ B1a cells in aged Blk+/− and Blk−/− spleens

Splenic $CD138^{+}$ B1a cells have been identified as natural IgM-producing cells (39) and can differentiate into IgG-producing B1a cells (44). Thus, we examined whether class-switched or IgG-secreting splenic B1a cells are increased in aged *Blk*+/− and *Blk*−/− mice. Given that class switch recombination (CSR) is applied to BCR class switching in B1 cells, $IgM^{lo/-}$ gated cells therefore contain class-switched cells. We modified the staining and gating strategy from Rothstein's and Herzenberg's groups (39, 44) and characterized splenic IgM^{hi} $CD138^{+}$ B1a cells as $IgM^{hi}IgD^{int/lo}B220^{int/hi}CD5^{int}CD43^{+}CD138^{+}$, while splenic $IgM^{lo/-}$ $CD138^{+}$ B1a cells were characterized as $IgM^{lo/-}IgD^{int/lo}B220^{int/hi}CD5^{int}$ $CD43^{+}CD138^{+}$ (Figure 3A). Splenic $IgM^{lo/-}$ $CD138^{+}$ B1a cells from aged *Blk*−/− mice, but to a lesser

extent from *Blk*+/− mice, had significant increase of $IgM^{lo/-}$ $CD138^{+}$ B1a cells compared to *Blk*+/+ mice. Conversely, *Blk* genotypes did not affect the absolute numbers of splenic IgM^{hi} $CD138^{+}$ B1a cells (Figure 3A & 3B). Sorted splenic $IgM^{lo/-}$ $CD138^{+}$ B1a cells preferentially differentiated into IgG-secreting cells in an ELISPOT assay, whereas sorted splenic IgM^{hi} $CD138^{+}$ B1a cells preferentially retained IgM-secreting capacities, using either *Blk*+/+ (Figure 3C) or *Blk*+/− and *Blk*−/− splenocytes (Figure S4A & S4D). Taken together, these results suggest that aged *Blk* deficiency increased the pool of splenic B1a cells that have the capacity to produce class-switched IgG.

Blk+/− and Blk−/− mice have infiltrating B1a cells in the inflamed kidneys

It is reported that infiltrated B1a cells in inflamed kidneys contribute to nephritis in NZB/W F1 mice (26, 38). We investigated whether the amounts of infiltrated B1a cells in the kidney correlated with the development of nephritis in *Blk*+/− and *Blk*−/− mice. Due to impaired CD23 surface staining from collagenase-treated kidney samples (data not shown), and because we found highest expression level of β1-integrin/VLA-4 on splenic B1a cells (B1a II, Figure S3A) among different B cell subsets (Figure S3C), we introduced β1-integrin/VLA-4 as a new marker to characterize B1a cells.

B1a-like cells were characterized as $CD19^{+}CD21^{int/lo}CD5^{+}CD43^{+}VLA4^{+}$ in splenocytes, regardless of the IgM expression level. Increased splenic B1a-like cells in aged *Blk*+/− and *Blk*−/− was confirmed (Figure 4A). So with confidence, the same parameters were applied to isolated leukocytes from kidneys. The data showed that few B1a-like cells infiltrate the kidneys of young female mice. Instead, an increased percentage of B1a-like cells were recruited into the kidneys of aged mice (Figure 4B). More importantly, there was a significantly increased frequency and absolute numbers of infiltrating B1a-like cells in kidneys from aged *Blk*+/− and *Blk*−/− mice, compared to aged *Blk*+/+ mice (Figure 4A & 4B). In contrast, infiltration of total $CD19^{+}$ B cells was not affected by *Blk* genotypes in aged mice (Figure 4C). The data demonstrated that B1a cell recruitment into inflamed kidneys is enhanced due to reduced or lost *Blk* expression. In agreement with this finding, the increase of infiltrating B1a cells into kidneys correlated with lupus nephritis development in aged females.

Carriers of the human BLK risk alleles of SNP rs2736340 have increased B1-like cells and higher levels of IgG anti-dsDNA antibodies in peripheral blood

We next examined if we observed a similar phenomenon in healthy carriers with risk alleles of the human *BLK* gene known to associate with reduced mRNA of *BLK*. Allele T of SNP rs2736340 in the BLK promoter region is associated with SLE risk and with low expression of BLK mRNA (3). In agreement with previous reports (3, 13), carriers of the CC-allele showed relatively higher mRNA expression levels of *BLK* than CT- or TT-risk allele carriers (Figure 5A). According to Griffin et al. (33) and recommended modifications (31, 32), we characterized human peripheral blood B1-like cells as $CD19^{+}CD3^{-}CD20^{+}CD43^{+}CD27^{+}$ (Figure 5B). Most of B1-like cells are $CD70^{-}$ (94.5%, Figure 5B) as described in Griffin et al (30). Consistent with highly expressed VLA-4 on murine B1a cells, the majority of human B1-like cells also expressed higher level of VLA-4 than B2 cells ($CD19^{+}CD20^{+}CD43^{-}$) (Figure S3D). Importantly, TT-risk allele carriers had increased

percentages of B1-like cells in PBMCs, compared to donors with CT and CC genotypes (Figure 5C). There was an inverse correlation between *BLK* mRNA expression and B1-like cell frequency (Figure 5D). While no difference between genotypes was detected in total IgM and IgG antibodies in serum (Figure 5E), we observed a significant increase in the level of IgG anti-dsDNA antibodies in CT- and TT-risk allele carriers, compared to CC-allele carriers, even if they were still lower than those detected in the sera of SLE patients (Figure 5E). Taken together, healthy individuals bearing *BLK* TT-risk allele have more B1-like cells in peripheral blood and higher levels of IgG anti-dsDNA antibodies in serum associated with low expression of *BLK* mRNA as compared to individuals bearing CT and CC alleles.

Presence of B1-like cells in kidney biopsies of human lupus nephritis patients

We analyzed biopsies from 13 SLE patients with lupus nephritis for the presence of B1-like cells in inflamed kidneys (Table 1). CD20 and CD43 were used as markers in the immunofluorescence staining of paraffin kidney sections, and nuclei were stained with DAPI for better visualization. $CD20^{-}CD43^{+}$ (T cells) and $CD20^{+}CD43^{-}$ cells (B cells) were detectable in the human kidney biopsies, suggesting the presence of T and B cells, respectively, in the tubule or interstitium (Figure 6). $CD20^{+}CD43^{+}$ double-positive cells (yellow on merged images) were also observed and considered as B1-like cells. $CD20^{+}CD43^{+}$ B1-like cells accumulated mostly in the interstitium, but less (or fragmented) in the tubule, and were perfectly distinguishable from CD43 single positive T cells or CD20 single positive B cells (Figure 6). The areas where $CD20^{+}CD43^{+}$ B1-like cells were observed had clear foci of infiltration. Cells were not observed in the glomeruli. No B1-like cells were detected in kidney biopsies of healthy donors (Figure 6). Therefore, this is the first demonstration of the presence of B1-like cells ($CD20^{+}CD43^{+}$) in human lupus nephritis biopsies. We quantified the numbers of $CD20^{+}$ B cells, $CD43^{+}$ T cells, or $CD20^{+}CD43^{+}$ B1-like cells per 0.01 mm^2 in each immunofluorescently stained slide and the values are shown in Table 1. We did not observe differences in B1-like cell infiltration between *BLK* non-risk or risk allele carriers with nephritis (Table 1). Nevertheless, we observed a tendency of female SLE patients bearing *BLK* risk alleles to have an earlier age of nephritis onset (not SLE onset) as compared to those bearing *BLK* non-risk alleles (median values with [IQR]: 24.0 [19.8 – 33.0] vs. 41.5 [33.8 – 45.3], p=0.020, Mann-Whitney test) (Table 1).

Discussion

We describe that reduced genotype-dependent expression level of *BLK* in mouse and human clearly correlated with the increased presence of B1a cells in the mouse and with a similar increase of B1-like cell in the human. Moreover, we observed a clear increase of IgG anti-dsDNA antibodies in healthy individuals with *BLK* risk genotypes, particularly those homozygous for the risk alleles. In the mouse, we were able to follow the development of kidney disease. We observed that *Blk*-deficient mice showed a later onset kidney disease, and had an increased infiltration of B1a cells into kidneys, prior, or close to the appearance of histological kidney inflammation. Furthermore, aged *Blk*+/− and *Blk*−/− female mice had increased serum IgG anti-dsDNA antibodies, IgG immune complex and complement 3 (C3) depositions, supporting the development of lupus nephritis. In human, we observed the presence of B1-like cells in kidney biopsies of lupus nephritis patients. Probably due to the

small numbers of individuals and different stages of the renal disease, we were unable to detect a relationship between the presence of B1-like cells and *BLK* genotypes. Nevertheless, we did find a potential relationship with earlier onset of lupus nephritis. In such a case, *BLK* risk variants, added to other susceptibility genes involved, might contribute to earlier development of renal nephritis. The data also supports prior studies of genetic association between lupus nephritis and risk alleles of *BLK* (45, 46) using the same SNP we used here.

The most striking phenotype we observed in aged *Blk*+/− and *Blk*−/− mice was the IC-mediated GN. Hybrid strains between 129 and C57BL/6 mice, widely used to generate gene-targeted mice, are spontaneously predisposed to development of humoral autoimmunity with low levels of GN (47). *Blk* mice we used were backcrossed to C57BL/6 for nine generations and the *Blk* gene is located in chromosome 14, but not chromosomes 1, 4, or 7, that contain several loci of lupus susceptibility genes (48, 49). Importantly, we did observe our aged *Blk* +/− or *Blk*−/− mice showing typical autoimmune phenotypes, such as IC-mediated GN and anti-dsDNA IgG production with a gender-bias, but complete absence of autoimmune disorders in *Blk*+/+ littermates. This clearly indicated that the contribution to autoimmunity is derived from reduction or loss of *Blk*. Samuelson et al. reported that reduced expression of *Blk* enhanced nephrosis in *B6.lpr/lpr* mice, but failed to observe any obvious autoimmune symptoms in the *B6.Blk+/-* mice (17, 24). The aged group of female mice in our report is 1-yr-old, but they used 5- to 6-month-old mice. Moreover, our data showed that anti-dsDNA IgG antibodies were not detectable until 48-wk-old. Therefore, age is one of the critical elements for *Blk*+/− and *Blk*−/− mice to get lupus signs.

B1a cells are polyreactive or even autoreactive with low-affinity to antigens (28, 50). We confirmed the presence of increased PerC B1a cells in young female *Blk*−/− mice (24). The role of PerC B1a cells in lupus pathogenesis is largely unknown, because PerC B1a cells do not produce immunoglobulins (28, 29). Previous work has shown that serous cavities are reservoirs of B1 cells and that B1 cells can recirculate to secondary lymphoid organs and tissues (51, 52) to differentiate into natural IgM- (nIgM) (44) or even IgG-producing cells, for instance, upon infection (27). Even nIgM is produced from steady-state B1 cells in spleen and bone marrow (53). Thus, we argue that splenic B1a cells, but not PerC B1a cells, may contribute to lupus pathogenesis. Our data suggest that accumulation of B1a cells in the spleen and their ability to then differentiate into IgG-secreting cells in this proper microenvironment in *Blk*+/− and *Blk*−/− mice could be a plausible mechanism to initiate autoantibody production, followed by the initiation of lupus-related symptoms.

Recent reports have shown a high frequency of autoantibody-secreting cells and long-lived $CD138^+$ plasma cells within inflamed kidneys of NZB/W F1 lupus mice (26, 38). Furthermore, class-switched autoreactive B1a cells in the course of murine lupus or Type 1 diabetes are subsequently accumulated in the inflamed target organs (29, 54). We reasoned whether infiltrated B1a cells produce more autoreactive IgG antibodies in the kidneys of *Blk* +/− and *Blk*−/− mice, just like B1a cells did in the spleen. Surprisingly, we were unable to detect reasonable production of IgG antibodies by class-switched $CD138^+$ B1a cells and $CD138^+$ plasma cells isolated from the kidney with appropriate controls (Figure S4B- S4E). Due to abundant IgG production from $CD138^+$ splenic B1a cells, this suggests the

possibility that IgG autoantibodies that deposited in the kidney may be produced and recirculated by antibody-producing cells from the spleen. On the other hand, the infiltrated B1a-like cells in the inflamed kidneys may have alternative fates. These will need to be further investigated.

Appearance of autoantibodies secreted by autoreactive B cells is believed to play a role of as initiator or executor in autoimmune pathogenesis (54, 55). Our data clearly indicate that reduction of *Blk* expression increases the accumulation of splenic B1a cells from an early age and $CD138^+$ IgG-producing B1a cells in the spleen at old age in our mice, possibly supporting the reasons why the development of the disease occurred at a late age in these mice. We noticed that B1a and B1-like cells express higher levels of VLA-4 ($\alpha4\beta1$ integrins) (Figure S3C & S3D) and it has been reported also for CD43 (Figure 3 & 5) (56) and CD9 (57). Those adhesion molecules might either help B1a or B1-like cells to be retained in the peritoneal cavity or the spleen, or promote their migration into, and egress from, lymphoid organs (52). Highly expressed VLA-4 on B1a cells can bind to VCAM1 on follicular dendritic cells (FDCs), supporting a close interaction between B1a cells and FDCs (43, 58). It further suggests that autoantibody production from FDC-associated splenic B1a cells, a T-independent type of B cell activation (58), would act as initiator to form autoAg-containing ICs (auto-ICs). Then those auto-ICs displayed on FDCs (59, 60) may activate emerging autoreactive B2 cells and trigger T-dependent germinal center responses.

Ours is the first observation that $CD20^+CD43^+$ B1-like cells are found in the tubulointerstitial space of human lupus nephritis kidneys. The same distribution has been observed for infiltrating $CXCR3^+CD4^+$ T cells (61) or plasma cells (62) known to induce glomerulonephritis. In fact, we also observed $CD43^+$ T cells and $CD20^+$ B cells in the interstitium. How the infiltrated B1-like cells collaborate with different recruited immune cells to trigger nephritis is still largely unexplored. Previous data derived from the NZB/W F1 lupus-prone mice (26, 38) and our current observations from aged *Blk*+/− and *Blk*−/− mice suggest that B1-like cells could have a pathogenic role in the development of lupus kidney disease in the human.

Our research has identified the cellular alterations by which low *BLK*-expressing polymorphic variants contribute to lupus, with particular emphasis on the potentially pathogenic role of B1 cells. The new understanding of B1a/ B1-like cells and their contribution to autoimmunity could have broad implications in the regulation of immune responses in different diseases, from autoimmune diseases to infections.

Supplementary Material

Refer to Web version on PubMed Central for supplementary material.

Acknowledgments

We thank the team of the OMRF Image Core facility, OMRF Flow Cytometry Core facility and Biorepository and Pathology Shared Resource Facility at Icahn School of Medicine at Mount Sinai for their technical support. We also thank for discussion of Dr. Ryuji Iida for FACS analysis of B1 cells and technical guidance of Dr. Lori Garman for the ELISPOT assay. We thank Ashley Bell, Marina Kravtsova, Huining Da and Farideh Movafagh for taking care of the mouse colonies and their genotyping, and Maria José Luque for processing of human samples.

Funding was primarily obtained from the COBRE NIH project (GM103456-10), the Alliance for Lupus Research, the Instituto de Salud Carlos III (PI12/02558, PI10/0552) partly supported by European FEDER funds, and the Fundación Ramón Areces. Also, This work has received support from the EU/EFPIA Innovative Medicines Initiative Joint Undertaking PRECISESADS grant n° 115565.

References

1. Delgado-Vega A, Sanchez E, Lofgren S, Castillejo-Lopez C, Alarcon-Riquelme ME. Recent findings on genetics of systemic autoimmune diseases. Current opinion in immunology. 2010; 22:698–705. [PubMed: 20933377]
2. Boackle AS. Advances in lupus genetics. Curr Opin Rheumatol. 2013; 25:561–568. [PubMed: 23917156]
3. Hom G, Graham RR, Modrek B, Taylor KE, Ortmann W, Garnier S, Lee AT, Chung SA, Ferreira RC, Pant PV, Ballinger DG, Kosoy R, Demirci FY, Kamboh MI, Kao AH, Tian C, Gunnarsson I, Bengtsson AA, Rantapaa-Dahlqvist S, Petri M, Manzi S, Seldin MF, Ronnblom L, Syvanen AC, Criswell LA, Gregersen PK, Behrens TW. Association of systemic lupus erythematosus with C8orf13-BLK and ITGAM-ITGAX. N Engl J Med. 2008; 358:900–909. [PubMed: 18204098]
4. Ito I, Kawasaki A, Ito S, Hayashi T, Goto D, Matsumoto I, Tsutsumi A, Hom G, Graham RR, Takasaki Y, Hashimoto H, Ohashi J, Behrens TW, Sumida T, Tsuchiya N. Replication of the association between the C8orf13-BLK region and systemic lupus erythematosus in a Japanese population. Arthritis Rheum. 2009; 60:553–558. [PubMed: 19180478]
5. Yang W, Ng P, Zhao M, Hirankarn N, Lau CS, Mok CC, Chan TM, Wong RW, Lee KW, Mok MY, Wong SN, Avihingsanon Y, Lee TL, Ho MH, Lee PP, Wong WH, Lau YL. Population differences in SLE susceptibility genes: STAT4 and BLK, but not PXK, are associated with systemic lupus erythematosus in Hong Kong Chinese. Genes Immun. 2009; 10:219–226. [PubMed: 19225526]
6. Gregersen KP, Amos CI, Lee AT, Lu Y, Remmers EF, Kastner DL, Seldin MF, Criswell LA, Plenge RM, Holers VM, Mikuls TR, Sokka T, Moreland LW, Bridges SL Jr, Xie G, Begovich AB, Siminovitch KA. REL, encoding a member of the NF-kappaB family of transcription factors, is a newly defined risk locus for rheumatoid arthritis. Nat Genet. 2009; 41:820–823. [PubMed: 19503088]
7. Gourh P, Agarwal SK, Martin E, Divecha D, Rueda B, Bunting H, Assassi S, Paz G, Shete S, McNearney T, Draeger H, Reveille JD, Radstake TRDJ, Simeon CP, Rodriguez L, Vicente E, Gonzalez-Gay MA, Mayes MD, Tan FK, Martin J, Arnett FC. Association of the C8orf13-BLK region with systemic sclerosis in North-American and European populations. Journal of Autoimmunity. 2010; 34:155–162. [PubMed: 19796918]
8. Nordmark G, Kristjansdottir G, Theander E, Appel S, Eriksson P, Vasaitis L, Kvarnstrom M, Delaleu N, Lundmark P, Lundmark A, Sjowall C, Brun JG, Jonsson MV, Harboe E, Goransson LG, Johnsen SJ, Soderkvist P, Eloranta ML, Alm G, Baecklund E, Wahren-Herlenius M, Omdal R, Ronnblom L, Jonsson R, Syvanen AC. Association of EBF1, FAM167A(C8orf13)-BLK and TNFSF4 gene variants with primary Sjogren's syndrome. Genes Immun. 2011; 12:100–109. [PubMed: 20861858]
9. Lessard JC, Li H, Adrianto I, Ice JA, Rasmussen A, Grundahl KM, Kelly JA, Dozmorov MG, Miceli-Richard C, Bowman S, Lester S, Eriksson P, Eloranta M-L, Brun JG, Goransson LG, Harboe E, Guthridge JM, Kaufman KM, Kvarnstrom M, Jazebi H, Graham DSC, Grandits ME, Nazmul-Hossain ANM, Patel K, Adler AJ, Maier-Moore JS, Farris AD, Brennan MT, Lessard JA, Chodosh J, Gopalakrishnan R, Hefner KS, Houston GD, Huang AJW, Hughes PJ, Lewis DM, Radfar L, Rohrer MD, Stone DU, Wren JD, Vyse TJ, Gaffney PM, James JA, Omdal R, Wahren-Herlenius M, Illei GG, Witte T, Jonsson R, Rischmueller M, Ronnblom L, Nordmark G, Ng W-F, for UKPSsSR, Mariette X, Anaya J-M, Rhodus NL, Segal BM, Scofield RH, Montgomery CG, Harley JB, Sivils KL. Variants at multiple loci implicated in both innate and adaptive immune responses are associated with Sjogren's syndrome. Nat Genet. 2013; 45:1284–1292. [PubMed: 24097067]
10. Yin H, Borghi MO, Delgado-Vega AM, Tincani A, Meroni PL, Alarcon-Riquelme ME. Association of STAT4 and BLK, but not BANK1 or IRF5, with primary antiphospholipid syndrome. Arthritis Rheum. 2009; 60:2468–2471. [PubMed: 19644876]
11. Miller FW, Cooper RG, Vencovsky J, Rider LG, Danko K, Wedderburn LR, Lundberg IE, Pachman LM, Reed AM, Ytterberg SR, Padyukov L, Selva-O'Callaghan A, Radstake TR,

Isenberg DA, Chinoy H, Ollier WE, O'Hanlon TP, Peng B, Lee A, Lamb JA, Chen W, Amos CI, Gregersen PK. Genome-wide association study of dermatomyositis reveals genetic overlap with other autoimmune disorders. Arthritis Rheum. 2013; 65:3239–3247. [PubMed: 23983088]

12. Lee Y-C, Kuo H-C, Chang J-S, Chang L-Y, Huang L-M, Chen M-R, Liang C-D, Chi H, Huang F-Y, Lee M-L, Huang Y-C, Hwang B, Chiu N-C, Hwang K-P, Lee P-C, Chang L-C, Liu Y-M, Chen Y-J, Chen C-H, Alliance TPID, Chen Y-T, Tsai F-J, Wu J-Y. Two new susceptibility loci for Kawasaki disease identified through genome-wide association analysis. Nat Genet. 2012; 44:522–525. [PubMed: 22446961]
13. Simpfendorfer RK, Olsson LM, Manjarrez Orduno N, Khalili H, Simeone AM, Katz MS, Lee AT, Diamond B, Gregersen PK. The autoimmunity-associated BLK haplotype exhibits cis-regulatory effects on mRNA and protein expression that are prominently observed in B cells early in development. Hum Mol Genet. 2012; 21:3918–3925. [PubMed: 22678060]
14. Guthridge JM, Lu R, Sun H, Sun C, Wiley GB, Dominguez N, Macwana SR, Lessard CJ, Kim-Howard X, Cobb BL, Kaufman KM, Kelly JA, Langefeld CD, Adler AJ, Harley IT, Merrill JT, Gilkeson GS, Kamen DL, Niewold TB, Brown EE, Edberg JC, Petri MA, Ramsey-Goldman R, Reveille JD, Vila LM, Kimberly RP, Freedman BI, Stevens AM, Boackle SA, Criswell LA, Vyse TJ, Behrens TW, Jacob CO, Alarcon-Riquelme ME, Sivils KL, Choi J, Joo YB, Bang SY, Lee HS, Bae SC, Shen N, Qian X, Tsao BP, Scofield RH, Harley JB, Webb CF, Wakeland EK, James JA, Nath SK, Graham RR, Gaffney PM. Two functional lupus-associated BLK promoter variants control cell-type- and developmental-stage-specific transcription. American journal of human genetics. 2014; 94:586–598. [PubMed: 24702955]
15. Delgado-Vega MA, Dozmorov MG, Quiros MB, Wu YY, Martinez-Garcia B, Kozyrev SV, Frostegard J, Truedsson L, de Ramon E, Gonzalez-Escribano MF, Ortego-Centeno N, Pons-Estel BA, D'Alfonso S, Sebastiani GD, Witte T, Lauwerys BR, Endreffy E, Kovacs L, Vasconcelos C, da Silva BM, Wren JD, Martin J, Castillejo-Lopez C, Alarcon-Riquelme ME. Fine mapping and conditional analysis identify a new mutation in the autoimmunity susceptibility gene BLK that leads to reduced half-life of the BLK protein. Ann Rheum Dis. 2012; 71:1219–1226. [PubMed: 22696686]
16. Laird RM, Laky K, Hayes SM. Unexpected role for the B cell-specific Src family kinase B lymphoid kinase in the development of IL-17-producing gammadelta T cells. J Immunol. 2010; 185:6518–6527. [PubMed: 20974990]
17. Samuelson EM, Laird RM, Papillion AM, Tatum AH, Princiotta MF, Hayes SM. Reduced B lymphoid kinase (Blk) expression enhances proinflammatory cytokine production and induces nephrosis in C57BL/6-lpr/lpr mice. PLoS ONE. 2014; 9:e92054. [PubMed: 24637841]
18. Cao W, Zhang L, Rosen DB, Bover L, Watanabe G, Bao M, Lanier LL, Liu YJ. BDCA2/Fc epsilon RI gamma complex signals through a novel BCR-like pathway in human plasmacytoid dendritic cells. PLoS Biol. 2007; 5:e248. [PubMed: 17850179]
19. Borowiec M, Liew CW, Thompson R, Boonyasrisawat W, Hu J, Mlynarski WM, El Khattabi I, Kim SH, Marselli L, Rich SS, Krolewski AS, Bonner-Weir S, Sharma A, Sale M, Mychaleckyj JC, Kulkarni RN, Doria A. Mutations at the BLK locus linked to maturity onset diabetes of the young and beta-cell dysfunction. Proc Natl Acad Sci U S A. 2009; 106:14460–14465. [PubMed: 19667185]
20. Castillejo-Lopez C, Delgado-Vega AM, Wojcik J, Kozyrev SV, Thavathiru E, Wu YY, Sanchez E, Pollmann D, Lopez-Egido JR, Fineschi S, Dominguez N, Lu R, James JA, Merrill JT, Kelly JA, Kaufman KM, Moser KL, Gilkeson G, Frostegard J, Pons-Estel BA, D'Alfonso S, Witte T, Callejas JL, Harley JB, Gaffney PM, Martin J, Guthridge JM, Alarcon-Riquelme ME. Genetic and physical interaction of the B-cell systemic lupus erythematosus-associated genes BANK1 and BLK. Ann Rheum Dis. 2012; 71:136–142. [PubMed: 21978998]
21. Aoki Y, Kim Y-T, Stillwell R, Kim TJ, Pillai S. The SH2 Domains of Src Family Kinases Associate with Syk. Journal of Biological Chemistry. 1995; 270:15658–15663. [PubMed: 7797565]
22. Bewarder N, Weinrich V, Budde P, Hartmann D, Flaswinkel H, Reth M, Frey J. In vivo and in vitro specificity of protein tyrosine kinases for immunoglobulin G receptor (FcgammaRII) phosphorylation. Mol Cell Biol. 1996; 16:4735–4743. [PubMed: 8756631]

23. Texido G, Su IH, Mecklenbrauker I, Saijo K, Malek SN, Desiderio S, Rajewsky K, Tarakhovsky A. The B-cell-specific Src-family kinase Blk is dispensable for B-cell development and activation. Mol Cell Biol. 2000; 20:1227–1233. [PubMed: 10648608]
24. Samuelson EM, Laird RM, Maue AC, Rochford R, Hayes SM. Blk haploinsufficiency impairs the development, but enhances the functional responses, of MZ B cells. Immunol Cell Biol. 2012; 90:620–629. [PubMed: 21894171]
25. Duan B, Morel L. Role of B-1a cells in autoimmunity. Autoimmun Rev. 2006; 5:403–408. [PubMed: 16890894]
26. Espeli M, Bokers S, Giannico G, Dickinson HA, Bardsley V, Fogo AB, Smith KG. Local renal autoantibody production in lupus nephritis. J Am Soc Nephrol. 2010; 22:296–305. [PubMed: 21088295]
27. Baumgarth N, Tung JW, Herzenberg LA. Inherent specificities in natural antibodies: a key to immune defense against pathogen invasion. Springer Semin Immunopathol. 2005; 26:347–362. [PubMed: 15633017]
28. Baumgarth N. The double life of a B-1 cell: self-reactivity selects for protective effector functions. Nat Rev Immunol. 2011; 11:34–46. [PubMed: 21151033]
29. Enghard P, Humrich JY, Chu VT, Grussie E, Hiepe F, Burmester GR, Radbruch A, Berek C, Riemekasten G. Class switching and consecutive loss of dsDNA-reactive B1a B cells from the peritoneal cavity during murine lupus development. Eur J Immunol. 2010; 40:1809–1818. [PubMed: 20333624]
30. Griffin DO, Holodick NE, Rothstein TL. Human B1 cells in umbilical cord and adult peripheral blood express the novel phenotype CD20+ CD27+ CD43+ CD70. J Exp Med. 2011; 208:67–80. [PubMed: 21220451]
31. Perez-Andres M, Grosserichter-Wagener C, Teodosio C, van Dongen JJ, Orfao A, van Zelm MC. The nature of circulating CD27+CD43+ B cells. J Exp Med. 2011; 208:2565–2566. [PubMed: 22184681]
32. Descatoire M, Weill JC, Reynaud CA, Weller S. A human equivalent of mouse B-1 cells? J Exp Med. 2011; 208:2563–2564. [PubMed: 22184680]
33. Griffin DO, Holodick NE, Rothstein TL. Human B1 cells are CD3-: A reply to “A human equivalent of mouse B-1 cells?” and “The nature of circulating CD27+CD43+ B cells”. J Exp Med. 2011; 208:2566–2569. [PubMed: 22184682]
34. Reynaud CA, Weill JC. Gene profiling of CD11b(+) and CD11b(−) B1 cell subsets reveals potential cell sorting artifacts. J Exp Med. 2012; 209:433–434. [PubMed: 22412175]
35. Griffin DO, Quach T, Batliwalla F, Andreopoulos D, Holodick NE, Rothstein TL. Human CD11b+ B1 cells are not monocytes: A reply to “Gene profiling of CD11b+ and CD11b- B1 cell subsets reveals potential cell sorting artifacts”. J Exp Med. 2012; 209:434–436. [PubMed: 22412176]
36. Griffin DO, Rothstein TL. A small CD11b(+) human B1 cell subpopulation stimulates T cells and is expanded in lupus. J Exp Med. 2011; 208:2591–2598. [PubMed: 22110167]
37. Kraljevic K, Wong S, Fulcher DA. Circulating phenotypic B-1 cells are decreased in common variable immunodeficiency and correlate with immunoglobulin M levels. Clinical and experimental immunology. 2013; 171:278–282. [PubMed: 23379434]
38. Starke C, Frey S, Wellmann U, Urbonaviciute V, Herrmann M, Amann K, Schett G, Winkler T, Voll RE. High frequency of autoantibody-secreting cells and long-lived plasma cells within inflamed kidneys of NZB/W F1 lupus mice. Eur J Immunol. 2011; 41:2107–2112. [PubMed: 21484784]
39. Holodick NE, Vizconde T, Rothstein TL. Splenic B-1a Cells Expressing CD138 Spontaneously Secrete Large Amounts of Immunoglobulin in Naive Mice. Front Immunol. 2014; 5:129. [PubMed: 24734034]
40. Bagavant H, Tung KS. Failure of CD25+ T cells from lupus-prone mice to suppress lupus glomerulonephritis and sialoadenitis. J Immunol. 2005; 175:944–950. [PubMed: 16002693]
41. Pan ZJ, Maier S, Schwarz K, Azbill J, Akira S, Uematsu S, Farris AD. Toll-like receptor 7 (TLR7) modulates anti-nucleosomal autoantibody isotype and renal complement deposition in mice exposed to syngeneic late apoptotic cells. Ann Rheum Dis. 2010; 69:1195–1199. [PubMed: 19674980]

42. Yenson V, Baumgarth N. Purification and immune phenotyping of B-1 cells from body cavities of mice. Methods Mol Biol. 2014; 1190:17–34. [PubMed: 25015270]
43. Wen L, Shinton SA, Hardy RR, Hayakawa K. Association of B-1 B cells with follicular dendritic cells in spleen. J Immunol. 2005; 174:6918–6926. [PubMed: 15905534]
44. Yang Y, Tung JW, Ghosn EE, Herzenberg LA. Division and differentiation of natural antibody-producing cells in mouse spleen. Proc Natl Acad Sci U S A. 2007; 104:4542–4546. [PubMed: 17360560]
45. Richman IB, Taylor KE, Chung SA, Trupin L, Petri M, Yelin E, Graham RR, Lee A, Behrens TW, Gregersen PK, Seldin MF, Criswell LA. European genetic ancestry is associated with a decreased risk of lupus nephritis. Arthritis Rheum. 2012; 64:3374–3382. [PubMed: 23023776]
46. Bolin K, Sandling JK, Zickert A, Jonsen A, Sjowall C, Svenungsson E, Bengtsson AA, Eloranta ML, Ronnblom L, Syvanen AC, Gunnarsson I, Nordmark G. Association of STAT4 polymorphism with severe renal insufficiency in lupus nephritis. PLoS ONE. 2013; 8:e84450. [PubMed: 24386384]
47. Carlucci F, Cortes-Hernandez J, Fossati-Jimack L, Bygrave AE, Walport MJ, Vyse TJ, Cook HT, Botto M. Genetic dissection of spontaneous autoimmunity driven by 129-derived chromosome 1 Loci when expressed on C57BL/6 mice. J Immunol. 2007; 178:2352–2360. [PubMed: 17277141]
48. Nguyen C, Limaye N, Wakeland EK. Susceptibility genes in the pathogenesis of murine lupus. Arthritis research. 2002; 3(4 Suppl):S255–S263. [PubMed: 12110145]
49. Morel L, Croker BP, Blenman KR, Mohan C, Huang G, Gilkeson G, Wakeland EK. Genetic reconstitution of systemic lupus erythematosus immunopathology with polycongenic murine strains. Proc Natl Acad Sci U S A. 2000; 97:6670–6675. [PubMed: 10841565]
50. Berland R, Wortis HH. Normal B-1a cell development requires B cell-intrinsic NFATc1 activity. Proc Natl Acad Sci U S A. 2003; 100:13459–13464. [PubMed: 14595020]
51. Kawahara T, Ohdan H, Zhao G, Yang YG, Sykes M. Peritoneal cavity B cells are precursors of splenic IgM natural antibody-producing cells. J Immunol. 2003; 171:5406–5414. [PubMed: 14607944]
52. Ha SA, Tsuji M, Suzuki K, Meek B, Yasuda N, Kaisho T, Fagarasan S. Regulation of B1 cell migration by signals through Toll-like receptors. J Exp Med. 2006; 203:2541–2550. [PubMed: 17060475]
53. Choi YS, Dieter JA, Rothaeusler K, Luo Z, Baumgarth N. B-1 cells in the bone marrow are a significant source of natural IgM. Eur J Immunol. 2012; 42:120–129. [PubMed: 22009734]
54. Diana J, Simoni Y, Furio L, Beaudoin L, Agerberth B, Barrat F, Lehuen A. Crosstalk between neutrophils, B-1a cells and plasmacytoid dendritic cells initiates autoimmune diabetes. Nat Med. 2013; 19:65–73. [PubMed: 23242473]
55. Liu Z, Davidson A. Taming lupus-a new understanding of pathogenesis is leading to clinical advances. Nat Med. 2012; 18:871–882. [PubMed: 22674006]
56. Oliveira FL, Chammas R, Ricon Ll, Fermino ML, Bernardes ES, Hsu DK, Liu F-T, Borojevic R, El-Cheikh MrC. Galectin-3 regulates peritoneal B1-cell differentiation into plasma cells. Glycobiology. 2009; 19:1248–1258. [PubMed: 19696234]
57. Won W-J, Kearney JF. CD9 Is a Unique Marker for Marginal Zone B Cells, B1 Cells, and Plasma Cells in Mice. The Journal of Immunology. 2002; 168:5605–5611. [PubMed: 12023357]
58. El Shikh MERM, El Sayed RM, Sukumar S, Szakal AK, Tew JG. Activation of B cells by antigens on follicular dendritic cells. Trends in immunology. 2010; 31:205–211. [PubMed: 20418164]
59. Heesters BA, Das A, Chatterjee P, Carroll MC. Do follicular dendritic cells regulate lupus-specific B cells? Molecular immunology. 2014; 62:283–288. [PubMed: 24636642]
60. Batista FD, Harwood NE. The who, how and where of antigen presentation to B cells. Nat Rev Immunol. 2009; 9:15–27. [PubMed: 19079135]
61. Enghard P, Humrich JY, Rudolph B, Rosenberger S, Biesen R, Kuhn A, Manz R, Hiepe F, Radbruch A, Burmester GR, Riemekasten G. CXCR3+CD4+ T cells are enriched in inflamed kidneys and urine and provide a new biomarker for acute nephritis flares in systemic lupus erythematosus patients. Arthritis Rheum. 2009; 60:199–206. [PubMed: 19116922]

62. Cassese G, Lindenau S, de Boer B, Arce S, Hauser A, Riemekasten G, Berek C, Hiepe F, Krenn V, Radbruch A, Manz RA. Inflamed kidneys of NZB / W mice are a major site for the homeostasis of plasma cells. Eur J Immunol. 2001; 31:2726–2732. [PubMed: 11536171]

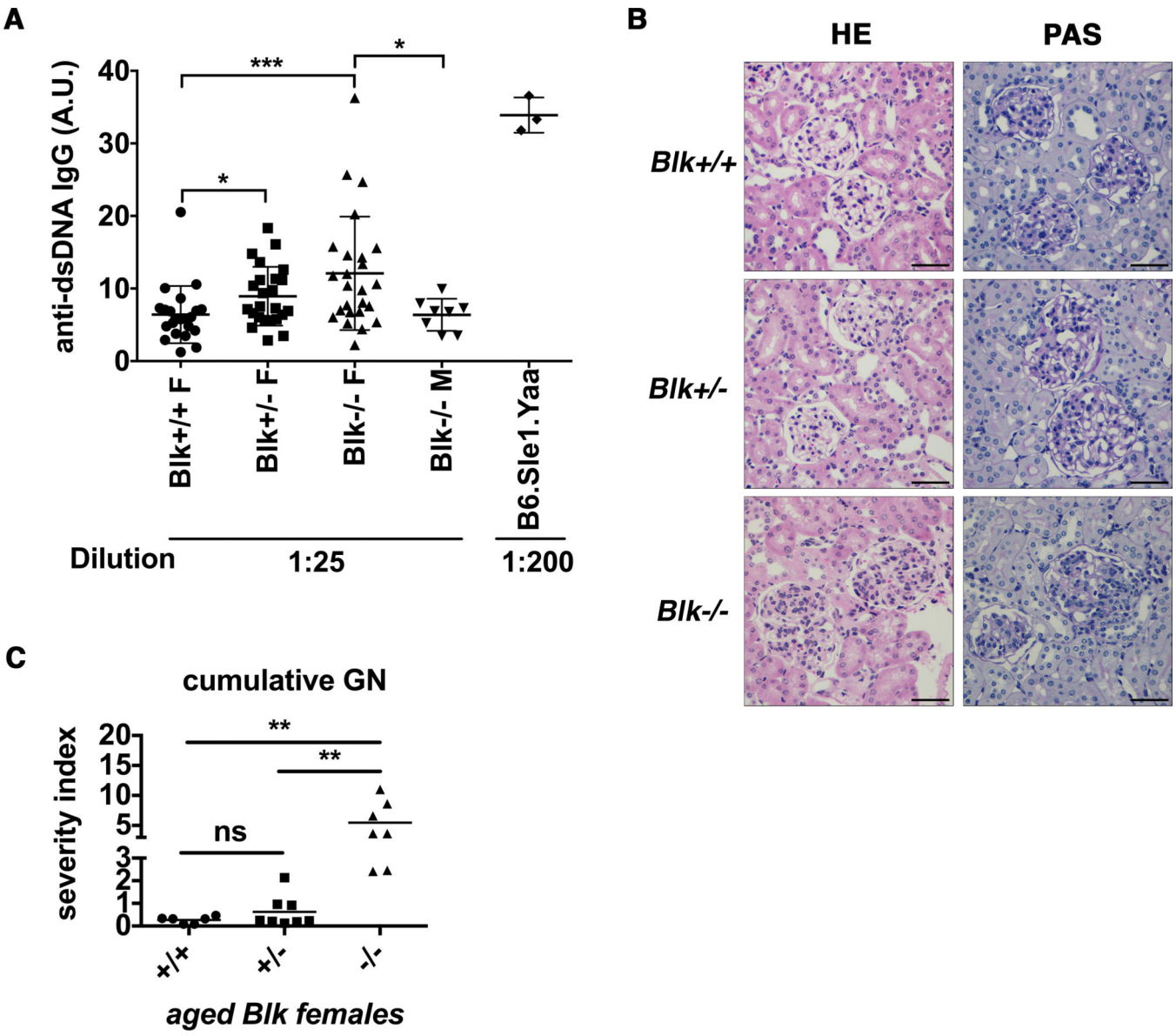

Figure 1. Aged female *Blk* deficient and -haploinsufficient mice show increased IgG anti-dsDNA and proliferative and chronic glomerulonephritis (GN)

(A) Sera from female and male mice with indicated *Blk* genotypes at 48-week of age were diluted 25 fold for ELISA measurement showing significantly increased anti-dsDNA IgG in *Blk*+/− and *Blk*−/− female mice (mean± SEM; ***p≤0.001, *p≤0.05, nonparametric *t* test). Serum from lupus-prone B6.Sle1.yaa males used as the positive controls was diluted 200 fold. Levels were expressed as arbitrary units (A.U.). Total aged mice analyzed: *Blk*+/+ F (n= 22), *Blk*+/− F (n= 24), *Blk*−/− F (n= 25), *Blk*−/− M (n= 8), B6.Sle1.yaa (n= 3). **(B)** Representative examples of glomeruli from *Blk*+/+, *Blk*+/−, and *Blk*−/− females at 55-wk stained with HE and periodic acid-Schiff stain (PAS). *Blk*−/− mice showed enlarged hypercellular glomeruli with inflammatory cell infiltrates. Black scale bars represented 100 μm. **(C)** The severity index of cumulative GN in female *Blk* mice at 48∼60-wk of age was determined through PAS-stained slides. Pathological changes were scored by two observers

blinded to the genotypes. Cumulative GN score is the summary of acute and chronic GN severity (mean; **p≤ 0.01, Kruskal-Wallis nonparametric test). Total aged mice analyzed: *Blk*+/+ (n= 6), *Blk*+/− (n= 8), *Blk*−/− (n= 7).

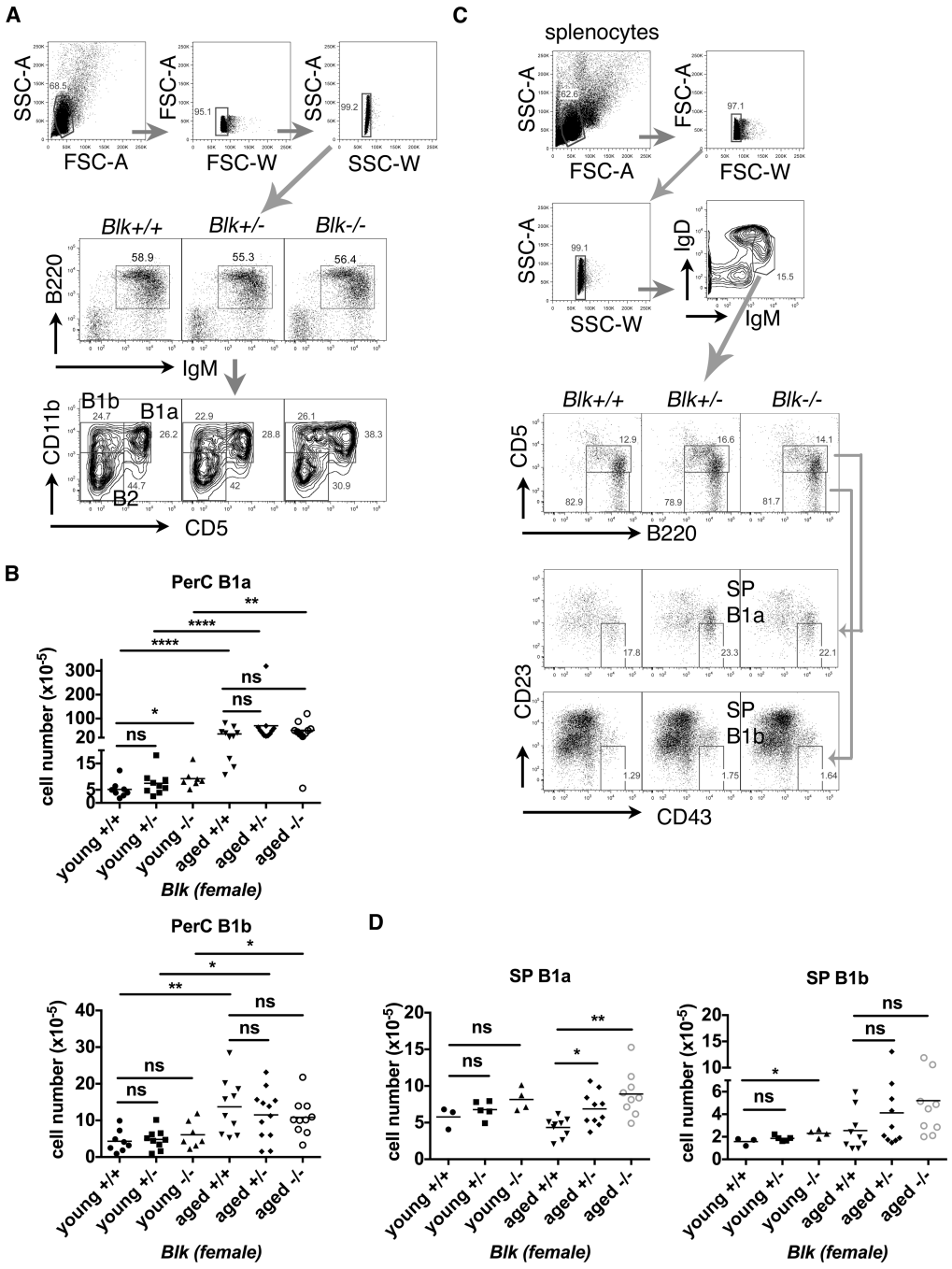

Figure 2. Flow cytometry analysis of peritoneal and splenic B1 cell subsets from young and aged female *Blk* mice

(A) Representative FACS plots of young female *Blk* mice from the same litter showed the gating strategies to discriminate debris and doublets in total peritoneal cells and for characterization of peritoneal B1a, B1b and B2 cells. Number represents the percentage within the gated populations. **(B)** The statistical plots show the absolute numbers of PerC B1a (upper) and B1b cells (lower) in young (8∼18-wk-old) and aged (52∼62-wk-old) *Blk* mice. Data pooled from 7 independent experimental cohorts of young mice and 4 of aged

mice. **(C)** Representative FACS plots of aged *Blk* mice from the same litter showed the gating strategies to discriminate debris and doublets in total splenocytes and to characterize splenic B1a and B1b cells. Number represents the percentage within the gated populations. **(D)** The statistical plots combine the absolute numbers of splenic (SP) B1a cells from cohorts of young (15∼18-wk-old) and aged (52∼61-wk-old) female *Blk* mice showing an increased accumulation of splenic B1a cells (left), but not of splenic B1b cells (right), in aged *Blk*+/− and *Blk*−/− mice. Data pooled from 3 independent experimental cohorts of young mice and 4 of aged mice. Both statistical plots in (B & D) are shown as mean with Kruskal-Wallis test (multiple comparison among *Blk* genotypes) or Mann-Whiney (young vs. aged) nonparametric test (*p≤0.05, **p≤0.01, ****p≤0.0001, ns>0.05).

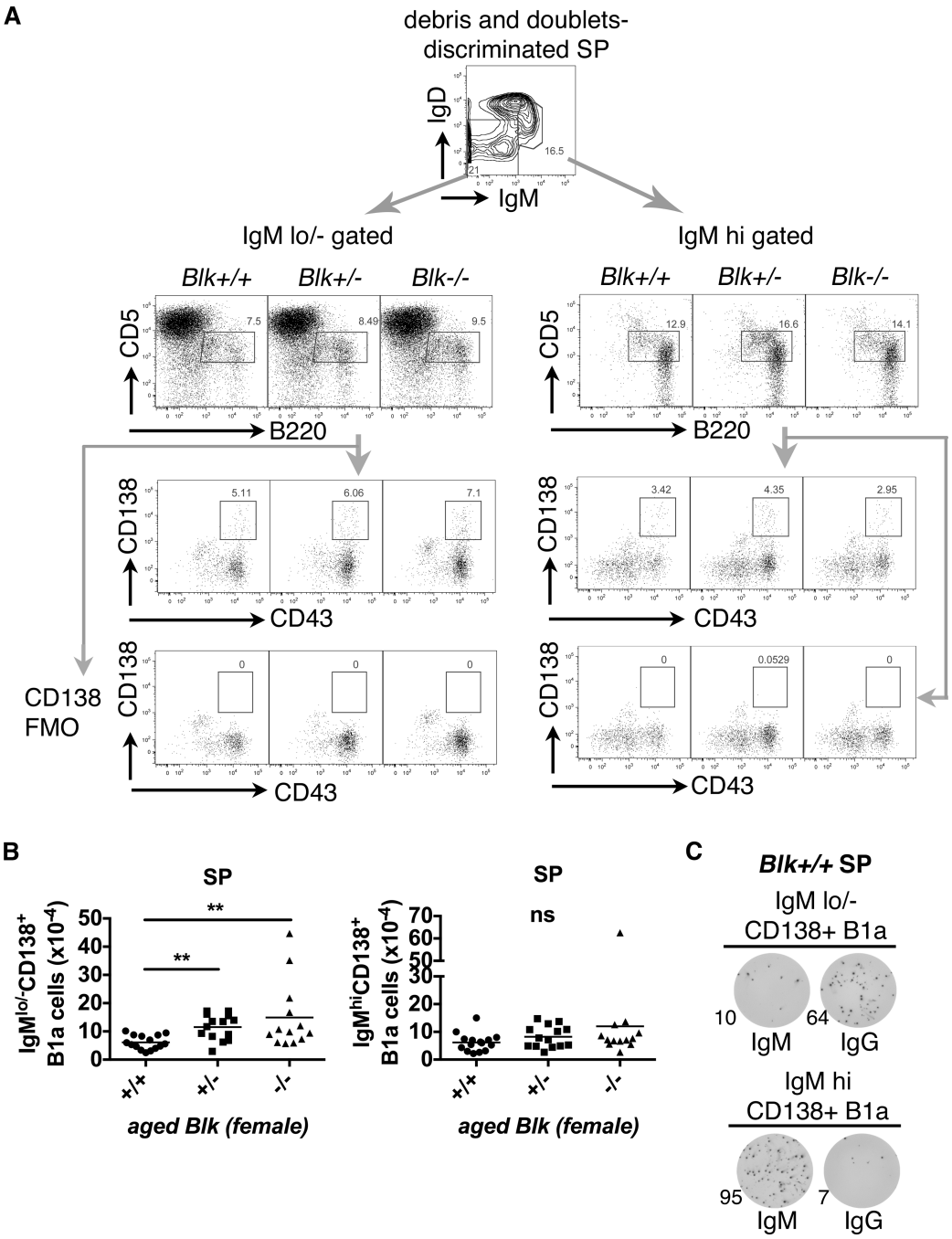

Figure 3. Increased number of class-switched CD138$^+$ splenic B1a cells from aged female *Blk*+/− and *Blk*−/− mice

(A) Representative FACS plots show the gating strategies for IgM$^{lo/-}$ and IgM^{hi}CD138$^+$ splenic B1a cells. The same strategy shown in Fig. 2C was used to discriminate debris and doublets in aged *Blk* mice. Number inside a plot represents percentage within gated population. Fluorescence minus one controls for CD138 (CD138 FMO) were included. **(B)** Total absolute number of splenic (SP) IgM$^{lo/-}$CD138$^+$ B1a cells (left) and IgM^{hi}CD138$^+$ B1a cells (right) presented in scattered dot plots (mean; ** p≤0.01, ns>0.05, Kruskal-Wallis

nonparametric test). Total aged female mice analyzed: *Blk*+/+ (n= 15), *Blk*+/− (n= 14), *Blk* −/− (n= 13), pooled from 6 independent experiments. **(C)** Representative IgM and IgG ELISPOT data from triplicates out of 2 independent experiments show that sorted $IgM^{lo/-}CD138^{+}$ B1a cells from a *Blk*+/+ spleen (SP) are IgG-producing cells, while sorted $IgM^{hi}CD138^{+}$ B1a cells are IgM-producing cells. The detailed sorting strategies are shown in Figure S4A. Number represents counted spots out of 1000 sort-purified cells within the well.

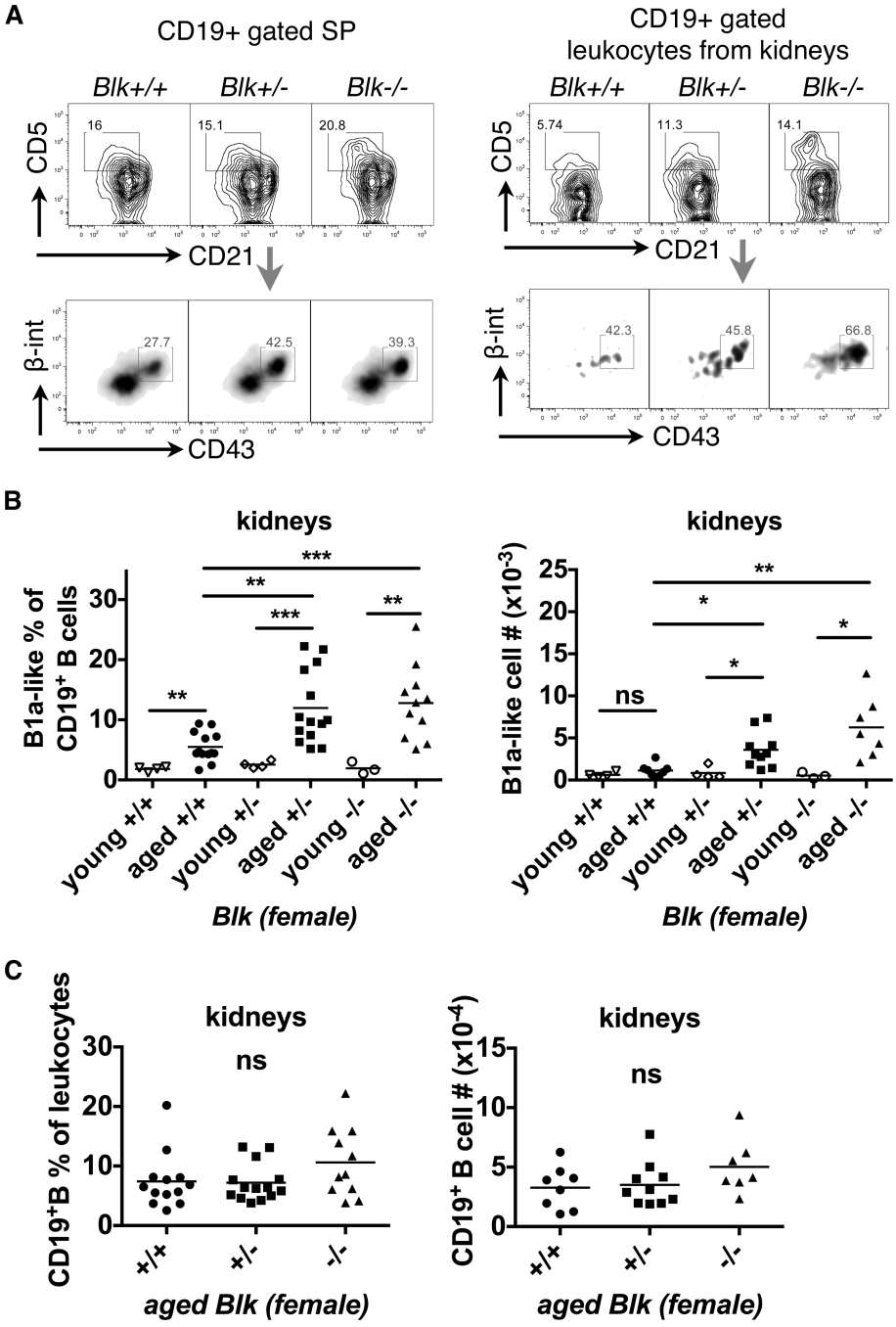

Figure 4. Reduced *Blk* expression accelerates the infiltration of B1a-like cells into the kidneys of aged female mice.

(A) Representative FACS plots show B1a-like cells ($CD19^{+}CD21^{int/lo}CD5^{+}CD43^{hi}\beta1\text{-integrin}^{int}$) from $CD19^{+}$ gated splenocytes (left panel) and leukocytes from kidneys (right panel) of aged *Blk* mice. The splenocytes and leukocytes from kidneys had undergone discrimination of debris and doublets and gating strategies were shown in the first 3 plots of Figure S4A and S4B. **(B)** The scattered dot plots combined the B1a-like cell frequency of $CD19^{+}$ B cells (left) and the absolute numbers of B1a-like cells (right) from kidneys of

young and aged female *Blk* mice. Kidneys from aged *Blk*+/− and *Blk*−/− mice have significantly increased B1a-like cells compared to ones from aged *Blk*+/+ mice. Total mice analyzed: young *Blk*+/+ (n= 4), young *Blk*+/− (n= 4), young *Blk*−/− (n= 3), pooled from 3 independent experiments; aged *Blk*+/+ (n= 13 for frequency; n= 8 for cell #), aged *Blk*+/− (n= 14 for frequency; n= 10 for cell #), aged *Blk*−/− (n= 11 for frequency; n= 7 for cell #), pooled from 5 independent experiments for the frequency and 3 for cell numbers. **(C)** Normal infiltration of $CD19^+$ B cells into kidneys from aged *Blk*+/+, *Blk*+/− and *Blk*−/− mice: the frequency of $CD19^+$ B cells in leukocytes (left) and absolute numbers of $CD19^+$ B cells (right) in kidneys. Both statistical plots (B & C) are shown as mean of Kruskal-Wallis (multiple comparison among *Blk* genotypes) or Mann-Whitney (young vs. aged) nonparametric test (*p≤0.05, **p≤0.01, ***p≤0.001, ns>0.05).

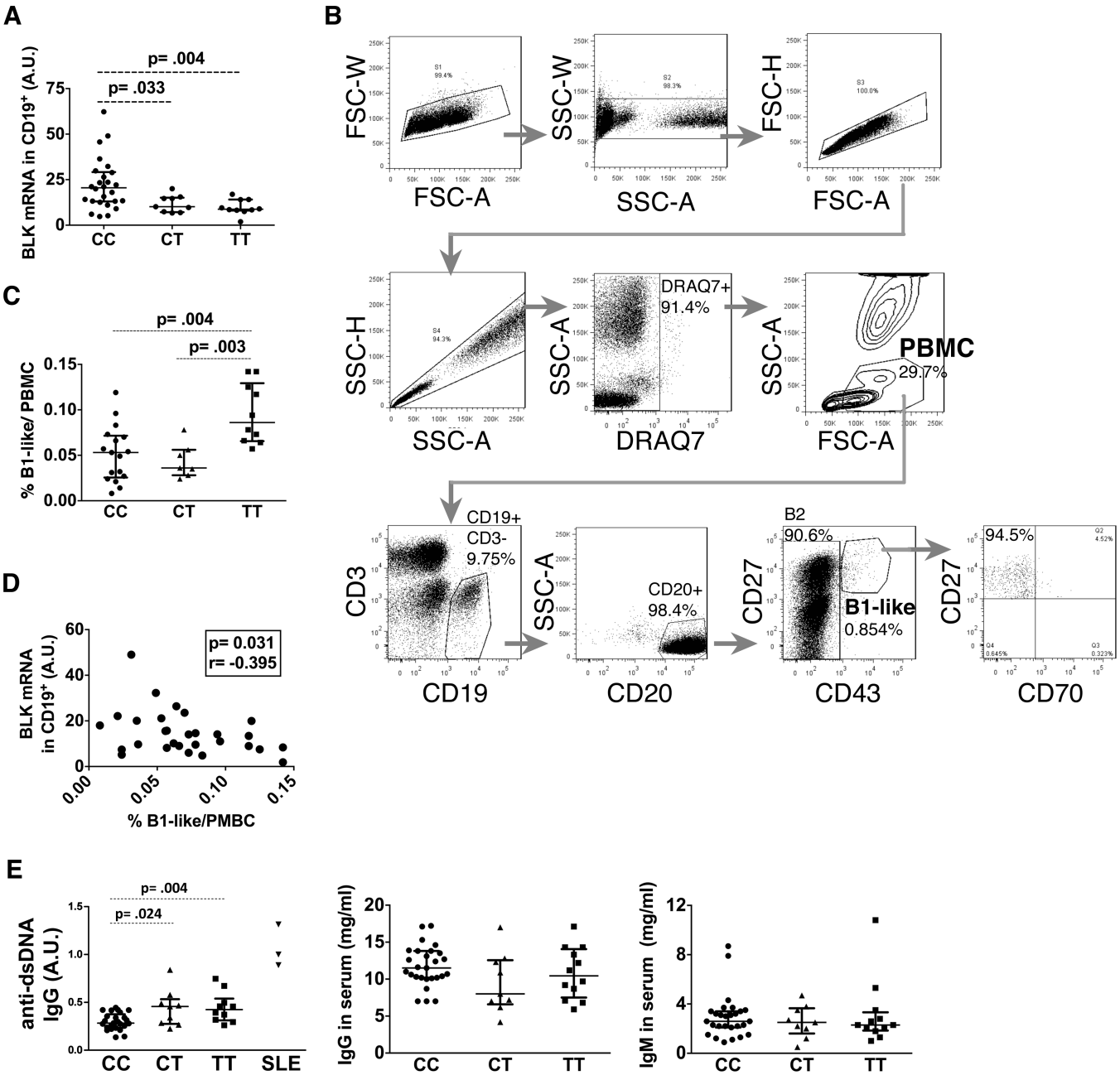

Figure 5. *BLK* risk allele carriers (rs2736340 TT) have increased B1-like cells in peripheral blood and IgG anti-dsDNA antibodies in serum

(A) The statistical plot represents *BLK* mRNA expression level in $CD19^+$ B cells from healthy individuals according to rs2736340 *BLK* genotypes. Total individuals analyzed: CC (n= 27), CT (n= 9), TT (n= 10). **(B)** Representative FACS plots of a healthy individual showing the gating strategy to characterize human PBMC-derived B1-like and B2 cells from erythrocyte-depleted whole blood. Dead cells were discriminated by DRAQ7 staining. **(C)** The statistical plot represents the frequency of $CD43^+CD27^+$ B1-like cells out of PBMCs from healthy individuals with differential *BLK* genotypes. Total individuals analyzed: CC (n= 17), CT (n= 7), TT (n= 10). **(D)** Correlation between *BLK* mRNA expression level in

$CD19^+$ B cells and % of B1-like cells from blood. p and r correlation values are calculated using Spearman test. **(E)** Statistical plots showing the serum levels of anti-dsDNA IgG autoantibodies in arbitrary unit (A.U.) (left), total IgG (middle), and total IgM (right) from the indicated genotype of healthy individuals and 3 SLE patients used as positive controls. Total healthy individuals analyzed: CC (n= 25), CT (n= 9), TT (n= 12). Statistical plots in (A, C & E) are shown as median ± IQR with Mann-Whitney nonparametric test.

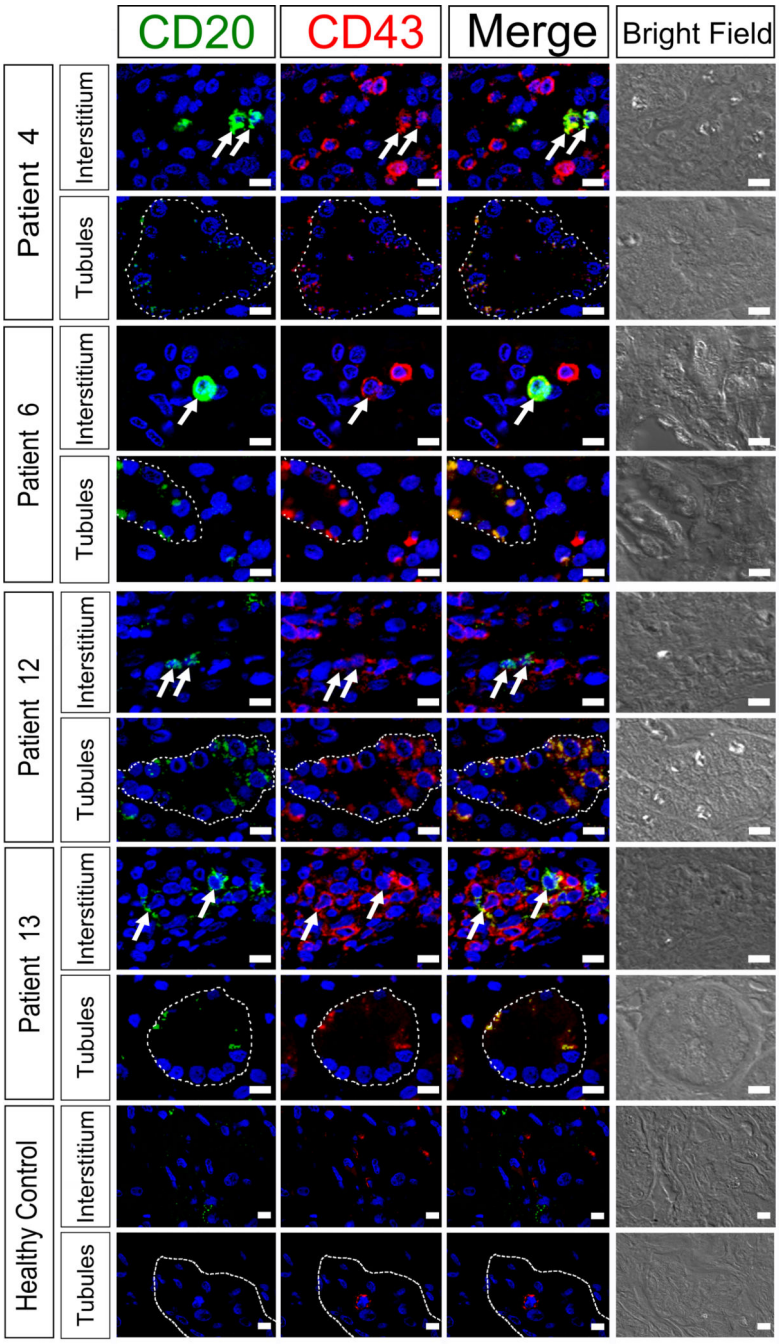

Figure 6. Presence of B1-like cells in the kidneys of SLE patients with lupus nephritis

Immunofluorescence for CD20 (green) and CD43 (red) was conducted to determine the presence of B1-like cells ($CD20^{+}CD43^{+}$ double positive) in SLE patients with lupus nephritis and a healthy control. In all patients examined B1-like cells were found regardless of their *BLK* genotype. The staining of four representative patients and one healthy control is shown. B1-like cells (arrows) present in the interstitium showed a strong $CD20^{+}CD43^{+}$ staining in the plasma membrane while B1-like cells in the tubule (dash line) show weaker staining, which is more dotted. In the interstitium, B1-like cells were mostly found in nests

of single CD20 and CD43 cells, respectively (Patient 4, 12, and 13). We did not observe cells inside glomeruli, but instead in clear foci of infiltration. The signal in the tubule varies from very strong (Patient 6, 12, and 13) to almost absent (Patient 4). Patient 4 and 6 are non-risk allele carriers, while patient 12 and 13 are risk allele carriers. White bars= 10 μm.

Table 1

Overview of patients with lupus nephritis included in the study

Patient no.	Age at biopsy/sex	median age with [IQR] in females	**_BLK_ SNP rs2736340 (C/T)	SLE nephritis	positive cells/0.01 mm²		
					CD20	CD43	CD20/CD43
1	42/F		non-risk	Class III	25.1	7.9	4.3
2	30/F	*40.83	non-risk	Class IV(G)	3.2	1.1	0.7
3	35/F	[33.8 – 45.3],	non-risk	Class IV(S)	2.8	22.3	4.3
#4	41/F	n=6	non-risk	Class IV(G)	0.1	1.5	0.2
5	55/F		non-risk	Class IV(G)	0.0	3.8	1.6
#6	42/F		non-risk	Class III	0.1	2.6	1.7
7	21/F		risk	Class IV(G)	0.3	4.9	0.4
8	16/F	*25.83	risk	Class III	0.0	0.6	0.0
9	39/F	[19.8 – 33.0],	risk	Class IV(S)	0.1	2.4	0.1
10	31/F	n=6	risk	Class IV(G)	0.1	1.3	0.0
11	22/F		risk	Class IV(G)	0.2	1.4	0.3
#12	26/F		risk	Class III	0.0	1.2	4.3
#13	59/M		risk	Class IV(G)/V	0.3	10.4	1.1

*p value = 0.020;

**non-risk: homozygous for CC; risk: homozygous for TT;

#Immunohistofluorescence staining data is shown in Figure 6.